

Transverse and spatial structure of light to heavy pseudoscalar mesons in light-cone quark model

Satyajit Puan^{1,*}, Navpreet Kaur^{1,†} and Harleen Dahiya^{1,‡}

¹ *Computational High Energy Physics Lab, Department of Physics,
Dr. B.R. Ambedkar National Institute of Technology, Jalandhar, 144008, India*

(Dated: October 11, 2024)

arXiv:2410.07596v1 [hep-ph] 10 Oct 2024

Abstract

In this work, we have investigated the transverse and spatial structure of light ($\pi^+(u\bar{d})$, $K^+(u\bar{s})$) and heavy ($\eta_c(c\bar{c})$, $\eta_b(b\bar{b})$, B and D) pseudoscalar mesons using the light-cone quark model. The transverse structure of these particles have been studied using the transverse momentum dependent parton distribution (TMDs). The leading twist unpolarized $f_1(x, \mathbf{k}_\perp^2)$ TMD has been solved using the quark-quark correlator. We have predicted the average momenta carried by the quark and antiquark of the considered mesons. For a complete description of mesons, we have also computed the leading twist unpolarized $H(x, 0, -t)$ generalized parton distribution (GPD). Further, electromagnetic form factors (EMFFs), along with gravitational form factors (GFFs) have been derived by taking the zeroth and first moments of the unpolarized GPD. These EMFFs are found to be compatible with available lattice simulation results. Further, we have also calculated the parton distribution functions (PDFs) for both the quarks and the antiquarks of these mesons. The PDF sum rule has also been verified.

Keywords: Heavy mesons, transverse momentum dependent parton distributions (TMDs), generalized parton distributions (GPDs), parton distribution functions (PDFs), distribution amplitudes (DAs).

I. INTRODUCTION

Understanding the complexity of a hadron structure in terms of its constituent partons such as quarks, gluons and sea quarks with fundamental rules of interactions among them is still a difficult task. After the discovery of quarks, it has been very fascinating to understand the internal structure of hadrons and the properties of constituents within it. The strong interactions among partons within the hadron and the hadronic matrix elements of quark-gluon field operators can be understood by using Quantum Chromodynamics (QCD) [1, 2]. The one-dimensional parton distribution functions (PDFs) are the simplest distribution functions carrying information about the longitudinal momentum fraction (x) carried by the constituent quark from its parent hadron [3–5]. PDFs are extracted from the deep inelastic scattering processes (DIS) in experiments [6, 7]. However, the transverse structure, spatial structure, quark densities, form factors, charge distributions etc of the quarks inside a hadron can not be accessed through the PDFs, the higher dimensional transverse momentum dependent parton distributions (TMDs) [8–11], generalized parton distributions

* puhansatyajit@gmail.com

† knavpreet.hep@gmail.com

‡ dahiyah@nitj.ac.in

(GPDs) [12–17], generalized transverse momentum dependent parton distributions (GTMDs) [18–20] are studied to achieve a complete description of a hadron. The three-dimensional (3D) TMDs are extended versions of PDFs with an addition of transverse structure. TMDs being function of longitudinal momentum fraction (x) and transverse momenta (\mathbf{k}_\perp) of an active quark, carry information on azimuthal asymmetries, spin densities, spin-orbit correlations, transverse spin effects, QCD confinement and factorization. TMDs can be extracted from Drell-Yan experiments, semi-inclusive deep inelastic scattering (SIDIS) processes [21], electron-positron annihilations [22, 23], Z^0/W^\pm productions [24] and DIS at high energy. However, TMDs do not carry any information on the spatial structure of quarks inside a hadron. Therefore, 3D GPDs play a pivotal role in describing the spatial structure of hadrons. GPDs are a function of longitudinal momentum fraction (x), skewness parameter (ζ) and transverse momentum transfer (Δ_\perp) between initial and final hadron. Skewness parameter ζ is the longitudinal momentum transferred between the initial and final parton. Elastic form factors (EFFs), mechanical properties, orbital angular momentum and physical properties of hadrons can be accessed through the GPDs [25–27] which can be extracted further directly from deeply virtual Compton scattering (DVCS) [28, 29] and deeply virtual meson production (DVMP) [30, 31].

In this work, we have investigated the unpolarized quark TMD and GPD for spin-0 pseudoscalar mesons. We have introduced these distribution functions for the heavy quarkonia, B and D -mesons along with the light pions and kaons. In case of spin-0 mesons, there are only two TMDs at the leading twist compared to 8 quark TMDs for the case of spin-1/2 nucleons [19, 32]. However in this case, we have considered only the time-reversal $f^q(x, \mathbf{k}_\perp^2)$ quark unpolarized TMD [33]. There is no experimental data available for pion TMDs, but there have been pion TMD extractions from Drell-Yan data [34] along with few lattice simulations observations [35, 36]. Various models such as NJL model [37], DSE Model, light-front holographic model [33], maximum entropy method [38], BSE model [39], spectator model [37] etc. have studied the pion TMDs successfully at the leading twist as well as for higher twists [37, 40]. Similarly, only single unpolarized PDF exists in the case of spin-0 pseudoscalar mesons. However, in case of spin-1/2 and 1 hadron [41], there are 3 and 4 PDFs respectively at the leading twist. For the case of pion, experimental data of unpolarized PDFs along with lattice simulations is available [42]. Even though no experimental data of the unpolarized PDFs for constituent quarks of kaon is available, some theoretical predictions along with model calculations are available [43, 44]. Analogously for heavy mesons, only theoretical predictions are available for TMDs and PDFs [45–48].

Further, there are two GPDs at the leading twist for the spin-0 mesons, out of which $H_M(x, \zeta, -t)$ is the chiral-even unpolarized GPD. No experimental data and very few lattice simulation results [49] are available for pion unpolarized GPD as far as our knowledge. There have been model calculations for pion and kaon GPDs in Refs. [50, 51]. This GPD is very special as it carries the information about electromagnetic form factors (EMFFs) and gravitational form factors (GFFs) of the mesons along with mechanical properties through D -term. In this current work, we have taken skewness parameter ζ as zero, therefore, the D -term vanishes. However, in the future we will try to calculate the mechanical properties like pressure, force and shear distribution through GPDs. The EMFF provide an insight of charge distribution inside a hadron. There have been some experimental data along with lattice simulations data for most of the mesons. Extraction of PDFs and EMFFs for light mesons is one of the important goals of the upcoming electron-ion collider (EIC) project [52]. However, these can not be directly probed in the experiment but can be accessed through Sullivan process. Further, COMPASS and AMBER experiment will provide more insight on the PDFs of pion and kaon in the recent time [53].

Valence quark distributions of spin-0 light and heavy pseudoscalar mesons in the form of TMDs, PDFs, GPDs and form factors has been calculated using light-cone quark model (LCQM) [54–59]. In case of heavy quarks, the higher Fock-state contributes very less compared to leading Fock-state [60]. So for this work, we have only considered the meson state as $|M\rangle = \sum |q\bar{q}\rangle\psi_{q\bar{q}}$. LCQM is a non-perturbative framework for understanding the internal structure and properties of hadrons like mass spectra, radiative decay, decay constant etc. It is gauge invariant and relativistic by nature. The advantage of LCQM is that it primarily focuses on the valence quarks of the hadrons and the valence quarks are the important constituents responsible for the overall structure and properties of hadrons. Even after proper QCD evolution of LCQM to perturbative limit, this model provides excellent results in describing the internal structure.

In this work, we have solved the quark-quark correlator for unpolarized valence quark TMDs and GPDs for light as well as heavy pseudoscalar mesons. As we are mainly focusing on the comparative analysis of light and heavy valence quarks, so we have not considered the gluon in the present work. We have obtained the overlap and explicit form of unpolarized $f_M^q(x, \mathbf{k}_\perp^2)$ quark TMD in the form of light front (LF) wave functions. We have considered both momentum space and spin wave functions for the LF wave functions. The collinear unpolarized TMD $f^q(x)$ quark PDF has been calculated by integrating the $f_M^q(x, \mathbf{k}_\perp^2)$ quark TMD over transverse momentum of valence quark. The pion and kaon valence quark PDFs have been evolved to $Q^2 = 16 \text{ GeV}^2$ through

DGLAP evolutions. These evolved PDFs have been compared with the available experimental data and other model predictions data. The average longitudinal momentum, transverse momentum and inverse momenta have also been calculated for all the mesons. To understand the spatial structure light as well as heavy pseudoscalar mesons, we have solved the GPDs correlator for valence quark at skewness $\zeta = 0$. The 3D structure of different mesons have been presented with respect to x and Δ_{\perp} . The 2D EMFFs have been extracted from the GPDs and compared with the available experimental data as well as lattice simulation data. These EMFFs found to be sync with both experimental and lattice simulation data.

The paper is arranged as follows. In Sec. II, we have discussed the LCQM along with the spin and momentum wave function in LF formalism. The input parameters and wave form for different mesons have also been discussed in this section. The TMDs and PDFs have been solved using the quark-quark correlator in Sec. III. The overlap form with explicit expressions for unpolarized quark TMD has been presented in this section. While in Sec. IV, we have presented the unpolarized GPDs and form factors derived from GPDs. We have finally summarized our work in Sec. VI.

II. METHODOLOGY

A. Light-cone quark model

While describing the hadrons relativistically in terms of quark and gluon degrees of freedom, the light-cone (LC) formalism offers an useful framework. By using the LC Fock-state expansion, one can express the mesonic wave function as [1, 61, 62]

$$|M\rangle = \sum |q\bar{q}\rangle\psi_{q\bar{q}} + \sum |q\bar{q}g\rangle\psi_{q\bar{q}g} + \sum |q\bar{q}gg\rangle\psi_{q\bar{q}gg} + \dots, \quad (1)$$

where $|M\rangle$ denotes the meson eigenstate. Since in this work we have not considered the higher Fock-state contribution [60], the hadron wave function based on the LC quantization of QCD using multi-particle Fock-state expansion can be expressed as [40, 63, 64]

$$|M(P, S_z)\rangle = \sum_{n, \lambda_i} \int \prod_{i=1}^n \frac{dx_i d^2\mathbf{k}_{\perp i}}{\sqrt{x_i} 16\pi^3} 16\pi^3 \delta\left(1 - \sum_{i=1}^n x_i\right) \delta^{(2)}\left(\sum_{i=1}^n \mathbf{k}_{\perp i}\right) \psi_{n/M}(x_i, \mathbf{k}_{\perp i}, \lambda_i) |n; \mathbf{k}_i^+, \mathbf{k}_{\perp i}, \lambda_i\rangle. \quad (2)$$

Here $|M(P, S_z)\rangle$ is the hadron eigenstate with $P = (P^+, P^-, P_\perp)$ as the meson's total momentum. λ_i and S_z are the helicity of the i -th constituent and longitudinal spin projection of the target respectively. $\mathbf{k}_i = (\mathbf{k}_i^+, \mathbf{k}_i^-, \mathbf{k}_{i\perp})$ is the i -th constituent momentum of the meson. Longitudinal momentum fraction carried by an active quark is defined as $x = \frac{k^+}{P^+}$. As we are dealing with lower Fock-state calculations, we have taken the minimal state description of Eq. (2) in the form of quark-antiquark and it can be expressed as

$$|M(P, S_z)\rangle = \sum_{\lambda_i, \lambda_j} \int \frac{dx d^2\mathbf{k}_\perp}{\sqrt{x(1-x)} 16\pi^3} \Psi_{S_z}(x, \mathbf{k}_\perp, \lambda_i, \lambda_j) |x, \mathbf{k}_\perp, \lambda_i, \lambda_j\rangle. \quad (3)$$

The four-vector momenta of the meson (P), constituent quark (k_1) and anti-quark (k_2) in the LC frame are respectively defined as

$$P \equiv \left(P^+, \frac{\mathcal{M}^2}{P^+}, \mathbf{0}_\perp \right), \quad (4)$$

$$k_1 \equiv \left(xP^+, \frac{\mathbf{k}_\perp^2 + m_q^2}{xP^+}, \mathbf{k}_\perp \right), \quad (5)$$

$$k_2 \equiv \left((1-x)P^+, \frac{\mathbf{k}_\perp^2 + m_{\bar{q}}^2}{(1-x)P^+}, -\mathbf{k}_\perp \right), \quad (6)$$

with \mathcal{M} being the invariant mass of the composite meson system defined in terms of its quark mass m_q and anti-quark mass $m_{\bar{q}}$ as

$$\mathcal{M}^2 = \frac{\mathbf{k}_\perp^2 + m_q^2}{x} + \frac{\mathbf{k}_\perp^2 + m_{\bar{q}}^2}{1-x}. \quad (7)$$

$\Psi_{S_z}(x, \mathbf{k}_\perp, \lambda_i, \lambda_j)$ in Eq. (3) is the LC meson wave function with different spin and helicity projections. It can be expressed as

$$\Psi_{S_z}(x, \mathbf{k}_\perp, \lambda_i, \lambda_j) = J_{S_z}(x, \mathbf{k}_\perp, \lambda_i, \lambda_j) \psi^M(x, \mathbf{k}_\perp). \quad (8)$$

Here $J_{S_z}(x, \mathbf{k}_\perp, \lambda_i, \lambda_j)$ and $\psi^M(x, \mathbf{k}_\perp)$ are the spin and momentum space wave functions of the mesons respectively. The momentum space wave function in Eq. (8) can be expressed using Brodsky-Huang-Lepage (BHL) [56, 63] as

$$\psi^M(x, \mathbf{k}_\perp) = A \exp \left[- \frac{\frac{\mathbf{k}_\perp^2 + m_q^2}{x} + \frac{\mathbf{k}_\perp^2 + m_{\bar{q}}^2}{1-x}}{8\beta^2} - \frac{(m_q^2 - m_{\bar{q}}^2)^2}{8\beta^2 \left(\frac{\mathbf{k}_\perp^2 + m_q^2}{x} + \frac{\mathbf{k}_\perp^2 + m_{\bar{q}}^2}{1-x} \right)} \right], \quad (9)$$

where A and β are the normalization constant and harmonic scale parameter of the mesons respectively. J_{S_z} in Eq. (9) is front-form spin wave function derived from the instant form by Melosh-Wigner rotation [50, 56, 63]. It is well known that to solve the ‘‘proton spin puzzle’’, it is essential

to comprehend the Melosh-Wigner rotation, which is fundamentally a relativistic phenomenon caused by the transverse motion of quarks inside the hadron [56, 63]. This transformation of instant form state $\Phi(T)$ and front form state $\Phi(F)$ is expressed as

$$\Phi_i^\uparrow(T) = -\frac{[\mathbf{k}_i^R \Phi_i^\downarrow(F) - (\mathbf{k}_i^+ + m_{q(\bar{q})}) \Phi_i^\uparrow(F)]}{\omega_i}, \quad (10)$$

$$\Phi_i^\downarrow(T) = \frac{[\mathbf{k}_i^L \Phi_i^\uparrow(F) + (\mathbf{k}_i^+ + m_{q(\bar{q})}) \Phi_i^\downarrow(F)]}{\omega_i}. \quad (11)$$

Here $\Phi(F)$ is a two-component Dirac spinor and $\mathbf{k}_i^{R(L)} = \mathbf{k}_i^1 \pm \mathbf{k}_i^2$. ω_i is defined as $\omega_i = 1/\sqrt{2\mathbf{k}_i^+ (\mathbf{k}_i^0 + m_{q(\bar{q})})}$. Now applying different momenta forms from Eqs. (4)-(6) in Melosh-Wigner rotation, the spin wave function is obtained in the form $\kappa_0^F(x, \mathbf{k}_\perp, \lambda_1, \lambda_2)$ coefficient as

$$J_{S_z}(x, \mathbf{k}_\perp, \lambda_i, \lambda_j) = \sum_{\lambda_1, \lambda_2} \kappa_0^F(x, \mathbf{k}_\perp, \lambda_1, \lambda_2) \Phi_1^{\lambda_1}(F) \Phi_2^{\lambda_2}(F). \quad (12)$$

These spin-wave function coefficients satisfy the following normalization relation

$$\sum_{\lambda_1, \lambda_2} \kappa_0^{F*}(x, \mathbf{k}_\perp, \lambda_1, \lambda_2) \kappa_0^F(x, \mathbf{k}_\perp, \lambda_1, \lambda_2) = 1. \quad (13)$$

Similarly, the same spin-wave function can be calculated using the proper vertex chosen for the meson [63, 65] as

$$J_{S_z}(x, \mathbf{k}_\perp, \lambda_i, \lambda_j) = \bar{u}(k_1, \lambda_1) \frac{\gamma_5}{\sqrt{2} \sqrt{\mathcal{M}^2 - (m_q^2 - m_{\bar{q}}^2)}} v(k_2, \lambda_2). \quad (14)$$

Here u and v are the Dirac spinors. Both the above methods give rise to same form of spin wave function. The spin wave function for pseudoscalar mesons ($S_z = 0$) with different helicities is expressed as [63]

$$\begin{cases} J_{(S_z=0)}(x, \mathbf{k}_\perp, \uparrow, \uparrow) = \frac{1}{\sqrt{2}} \omega^{-1}(-\mathbf{k}^L)(\mathcal{M} + m_q + m_{\bar{q}}), \\ J_{(S_z=0)}(x, \mathbf{k}_\perp, \uparrow, \downarrow) = \frac{1}{\sqrt{2}} \omega^{-1}((1-x)m_q + xm_{\bar{q}})(\mathcal{M} + m_q + m_{\bar{q}}), \\ J_{(S_z=0)}(x, \mathbf{k}_\perp, \downarrow, \uparrow) = \frac{1}{\sqrt{2}} \omega^{-1}(-(1-x)m_q - xm_{\bar{q}})(\mathcal{M} + m_q + m_{\bar{q}}), \\ J_{(S_z=0)}(x, \mathbf{k}_\perp, \downarrow, \downarrow) = \frac{1}{\sqrt{2}} \omega^{-1}(-\mathbf{k}^R)(\mathcal{M} + m_q + m_{\bar{q}}), \end{cases} \quad (15)$$

with $\omega = (M + m_q + m_{\bar{q}}) \sqrt{x(1-x)[M^2 - (m_q - m_{\bar{q}})^2]}$. The two-particle Fock-state in Eq. (3) can be written in the form of LC wave functions (LCWFs) with all possible helicities of its constituent

quark and anti-quark as

$$\begin{aligned}
|M(P^+, \mathbf{P}_\perp, S_z = 0)\rangle = & \int \frac{dx d^2\mathbf{k}_\perp}{2(2\pi)^3 \sqrt{x(1-x)}} [\Psi_{S_z=0}(x, \mathbf{k}_\perp, \uparrow, \uparrow) |xP^+, \mathbf{k}_\perp, \uparrow, \uparrow\rangle \\
& + \Psi_{S_z=0}(x, \mathbf{k}_\perp, \downarrow, \downarrow) |xP^+, \mathbf{k}_\perp, \downarrow, \downarrow\rangle + \Psi_{S_z=0}(x, \mathbf{k}_\perp, \downarrow, \uparrow) \\
& |xP^+, \mathbf{k}_\perp, \downarrow, \uparrow\rangle + \Psi_{S_z=0}(x, \mathbf{k}_\perp, \uparrow, \downarrow) |xP^+, \mathbf{k}_\perp, \uparrow, \downarrow\rangle]. \quad (16)
\end{aligned}$$

B. Input parameters and wave functions

For the numerical calculations in LCQM, we need only quark (antiquark) masses ($m_{q(\bar{q})}$) and harmonic scale parameter (β) as the input parameters. These parameters have been adopted following Refs. [40, 66] and have been presented in Table I. These parameters have been calculated by fitting meson masses for pure state [40, 66] and they provide excellent results for decay constant and DAs. For a complete descriptions of light and heavy quarks within a meson, we have taken $\pi^+(u\bar{d})$, $K^+(u\bar{s})$, $\eta_c(c\bar{c})$, $\eta_b(b\bar{b})$, $D^+(c\bar{d})$, $D_s(c\bar{s})$, $B^+(u\bar{b})$, $B_s(s\bar{b})$ and $B_c(c\bar{b})$ spin-0 mesons. In order to understand in detail the role of masses in the longitudinal momentum fraction carried by the parton, the momentum space wave functions $\psi^M(x, \mathbf{k}_\perp)$ from Eq. (9) have been plotted with respect to longitudinal momentum fraction x at transverse quark momenta $\mathbf{k}_\perp^2 = 0.5$ GeV for all the mesons in the left panel of Fig. 1. Momentum space wave functions of mesons with equal quark (antiquark) masses show symmetry about $x \longleftrightarrow (1-x)$. Mesons with a heavier antiquark show a shift of LCWF towards lower longitudinal momentum fraction (x) and have a maximum distribution in between $0 \leq x \leq 5$, whereas opposite trend of distribution is observed for meson with heavier quark. Mesons like B_c , B^+ , D^+ and D_s with light-heavy quark-antiquark pair shows higher peak distributions than other mesons. B -meson shows no distribution after $x \leq 0.6$ due to the presence of heavy b -anti-quark, while for the case of D -mesons it shows the trend below $x \leq 0.2$. In case of η_b meson, the distribution is higher than the η_c , however both have maximum distributions at $x = 0.5$ along with pion.

In the right panel of Fig. 1, we have plotted the momentum space wave function with respect to transverse momenta of quark (\mathbf{k}_\perp) at a fixed value of longitudinal momentum fraction ($x = 0.25$) and 0.5 respectively for different mesons. The wave function of pion vanishes after $\mathbf{k}_\perp = 1$ GeV very sharply when compared to the drop in the case of other mesons but has a higher maximum distributions at $x = 0.25$ as compared to the other mesons as seen in Fig. 1 (b). Similar observation can be made for the case of kaon in Fig. 1 (d). This clearly indicates that higher the mass of the

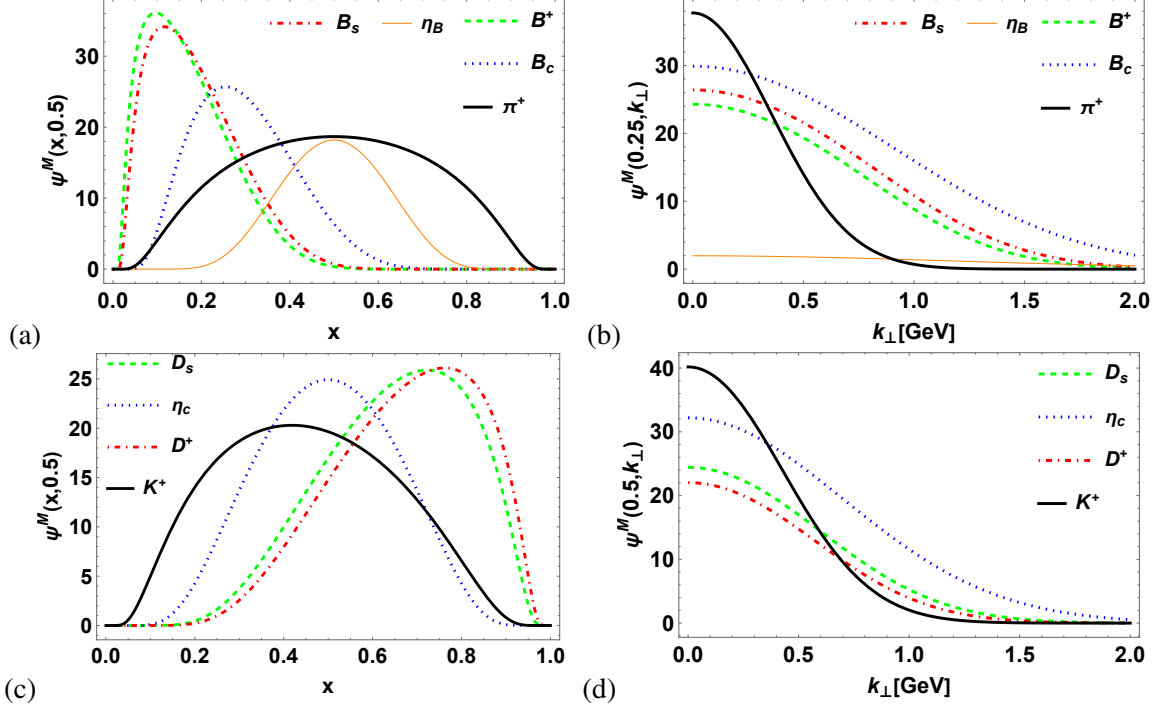


FIG. 1: (Color online) Momentum space wave function of light and heavy mesons have been plotted with longitudinal momentum fraction (x) at fixed value of transverse momentum ($\mathbf{k}_\perp = 0.5$ GeV) in the left panel, while in the right panel these mesons have been plotted with \mathbf{k}_\perp at fixed $x = 0.25$ and 0.5 respectively.

$m_{u(d)}$	m_s	m_c	m_b	β_{qq}	β_{qs}	β_{qc}	β_{cc}	β_{bb}	β_{sc}	β_{qb}	β_{sb}	β_{bc}
0.22	0.45	1.68	5.10	0.410	0.405	0.500	0.699	1.376	0.537	0.585	0.636	0.906

TABLE I: The constituent light quark masses m_q ($q = u, d$ and s), heavy quark masses m_Q ($Q = c$ and b) and harmonic scale parameter β are in unit of GeV. These parameters have been adopted from Ref. [40, 66]

meson, higher is the spread of the wave functions in the \mathbf{k}_\perp direction.

III. TRANSVERSE MOMENTUM PARTON DISTRIBUTION FUNCTIONS

For spin-0 pseudoscalar mesons, the valence quark unpolarized TMDs can be expressed through the quark-quark correlation function, which is defined as

$$f^q_M(x, \mathbf{k}_\perp^2) = \frac{1}{2} \int \frac{dz^- d^2 z_\perp}{2(2\pi)^3} e^{ix\bar{P}\cdot z} \left\langle M(P, \lambda') \left| \bar{\Theta} \left(-\frac{z}{2} \right) \mathcal{W}(-z/2, z/2) \gamma^+ \Theta \left(\frac{z}{2} \right) \right| M(P, \lambda) \right\rangle, \quad (17)$$

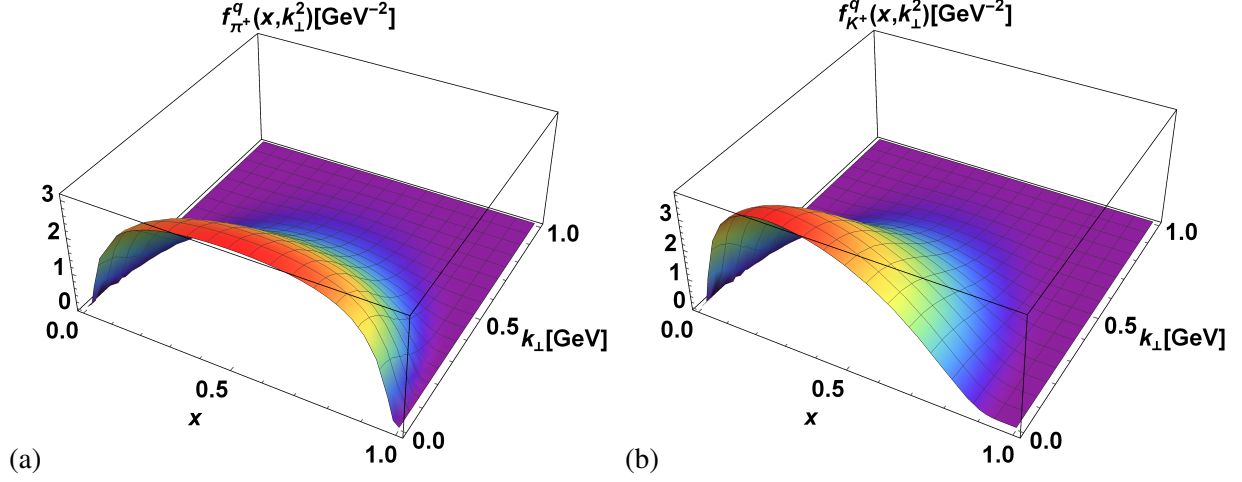


FIG. 2: (Color online) Unpolarized quark transverse momentum parton distribution function as a function of longitudinal momentum fraction x and transverse momentum \mathbf{k}_{\perp} of (a) pion and (b) kaon.

where $z = (z^+, z^-, z^{\perp})$ is the position four-vector. \bar{P} is the average momentum of initial and final state momentum of the meson. Θ represents the quark field operator at two different positions $-z/2$ and $z/2$. $\mathcal{W}(-z/2, z/2)$ is the Wilson line which preserves the gauge invariance of the bilocal quark field operators in the correlation functions [67] which has been taken as 1 in the present case. The function f_M^q describes the momentum distribution of unpolarized valence quark within a meson. For the polarized quark momentum distributions, we have to study the Boer-Mulders $h_1^{\perp}(x, \mathbf{k}_{\perp}^2)$ TMD [33]. The overlap form of unpolarized $f_M^q(x, \mathbf{k}_{\perp}^2)$ TMD in the form of LCWFs, as expressed in Eq. (8), are found to be

$$f_M^q(x, \mathbf{k}_{\perp}^2) = \frac{1}{16\pi^3} [|\Psi_{S_z=0}(x, \mathbf{k}_{\perp}, \uparrow, \uparrow)|^2 + |\Psi_{S_z=0}(x, \mathbf{k}_{\perp}, \downarrow, \downarrow)|^2 + |\Psi_{S_z=0}(x, \mathbf{k}_{\perp}, \downarrow, \uparrow)|^2 + |\Psi_{S_z=0}(x, \mathbf{k}_{\perp}, \uparrow, \downarrow)|^2]. \quad (18)$$

The explicit form of $f_M^q(x, \mathbf{k}_{\perp}^2)$ TMD by introducing space and spin wave functions can be expressed as

$$f_M^q(x, \mathbf{k}_{\perp}^2) = \frac{1}{16\pi^3} \left[(\mathcal{M} + m_q + m_{\bar{q}})^2 (\mathbf{k}_{\perp}^2 + (1-x)m_q + xm_{\bar{q}})^2 \right] \frac{|\psi^M(x, \mathbf{k}_{\perp})|^2}{\omega^2}. \quad (19)$$

For the present work, we have considered only the unpolarized quark TMD. This TMD has been plotted with respect to longitudinal momentum fraction (x) and transverse momenta of quark

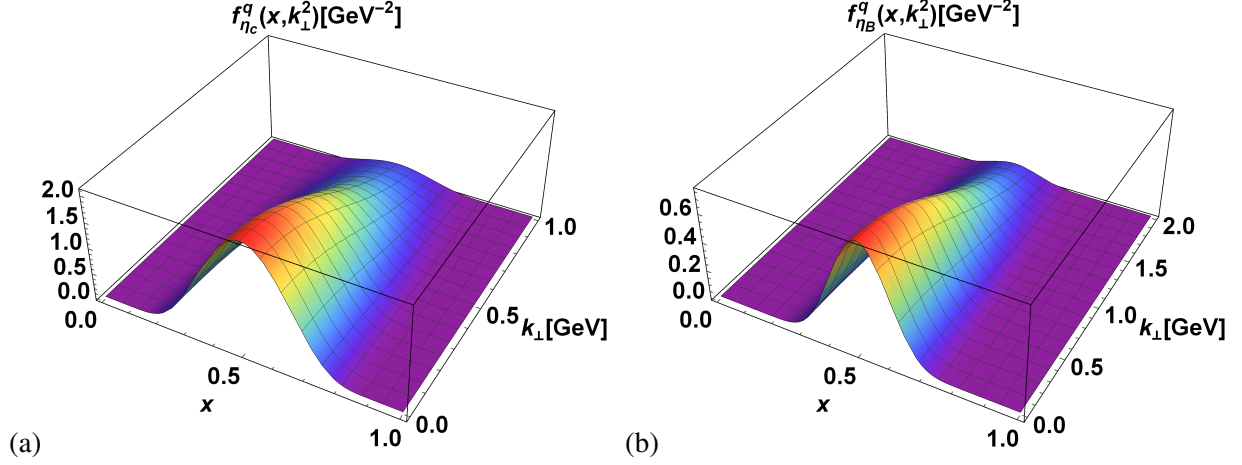


FIG. 3: (Color online) Unpolarized quark transverse momentum parton distribution function as a function of longitudinal momentum fraction x and transverse momentum \mathbf{k}_\perp of (a) η_c and (b) η_b mesons.

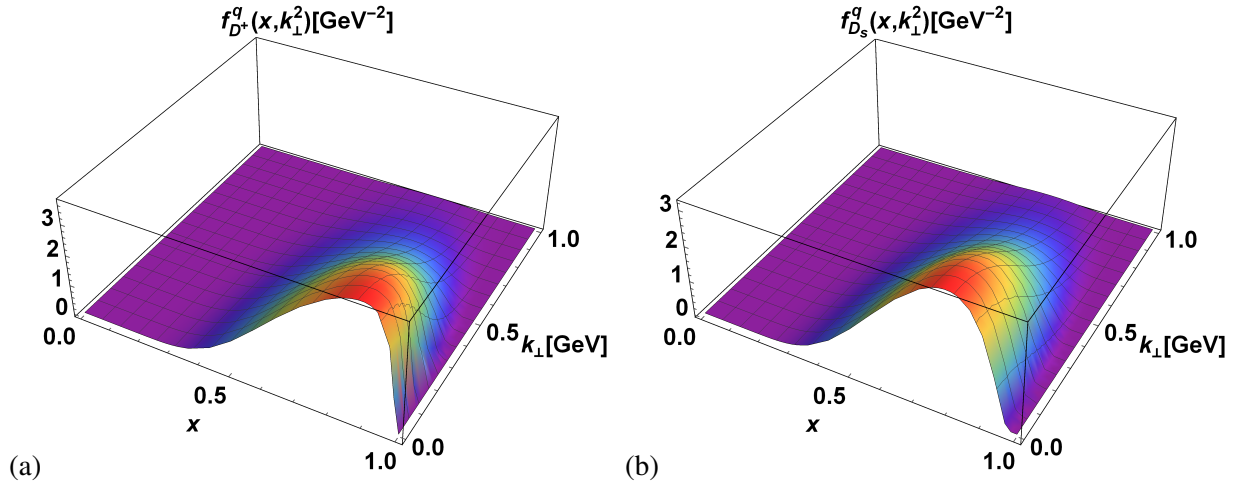


FIG. 4: (Color online) Unpolarized quark transverse momentum parton distribution function as a function of longitudinal momentum fraction x and transverse momentum \mathbf{k}_\perp of (a) D^+ and (b) D_s mesons.

(\mathbf{k}_\perp^2) for quark of light and heavy mesons in Figs. 2, 3, 4, and 5. For the case of pion (Fig. 2), the quark TMD distribution is spread over the entire x range and found to be a smooth decreasing function with increase in the transverse momentum \mathbf{k}_\perp (GeV) of the quark. However, in case of other mesons (Figs. 3, 4, and 5), the distributions are limited to certain range of x . It is

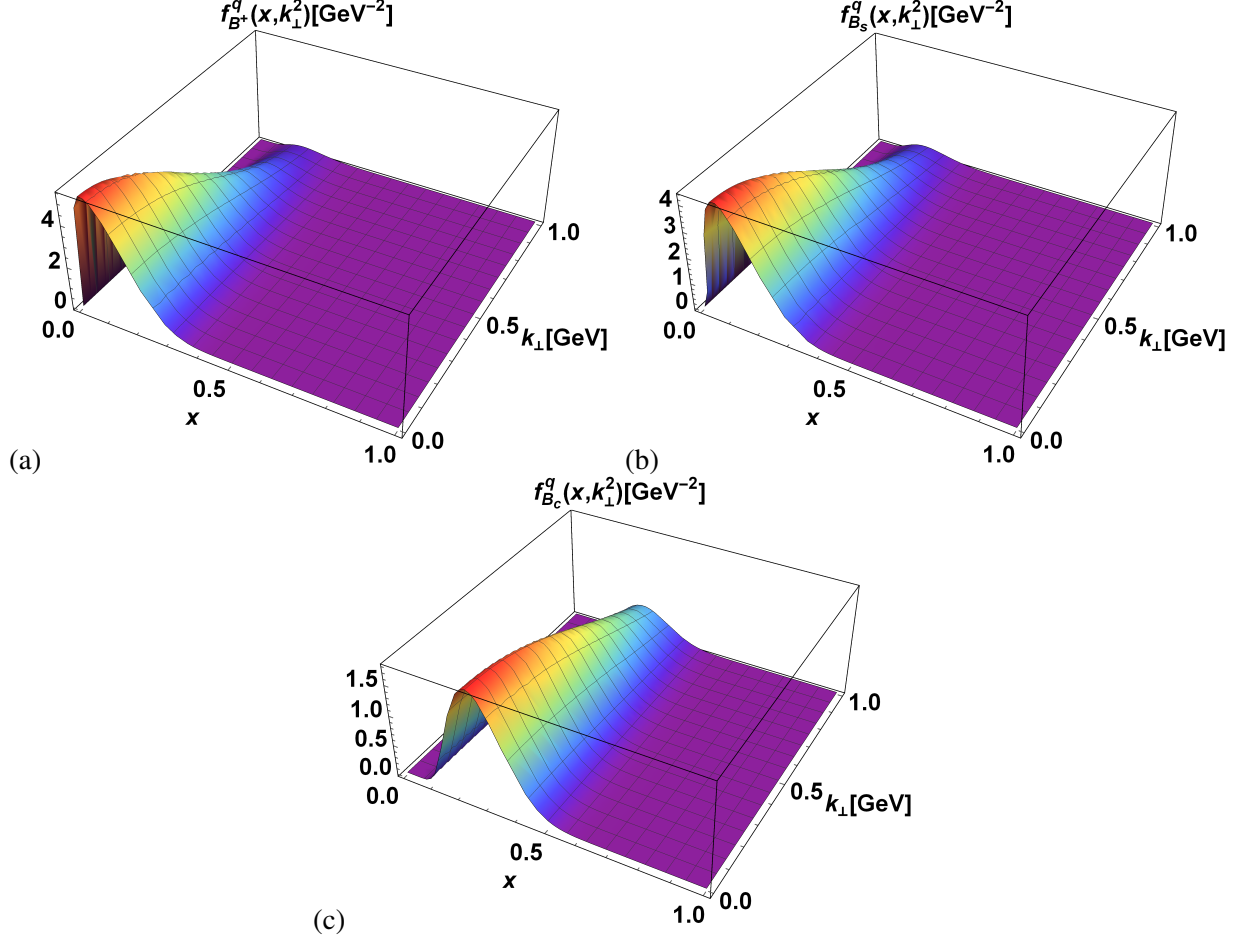


FIG. 5: (Color online) Unpolarized quark transverse momentum parton distribution function as a function of longitudinal momentum fraction x and transverse momentum \mathbf{k}_\perp of (a) B^+ (b) B_s , and (c) B_c mesons.

observed that unpolarized quark TMD obeys the positivity constrain $f_M^q(x, \mathbf{k}_\perp^2) \geq 0$ for all the mesons [40, 68, 69]. Quark TMDs with lighter quark mass show a shift of distribution towards lower value of x , while the trend is opposite for the case of heavy quark TMDs. Further, the heavy meson distributions decrease slowly with increase in \mathbf{k}_\perp as compared to that in the light mesons. This kind of property has also been observed in the BS model [45], algebraic model [46] and in DSE model [70]. Mesons with equal quark and antiquark mass show a symmetry about $x \leftrightarrow (1-x)$ with a peak distribution at $x = 0.5$. Quark TMD of heavy mesons show narrow x dependence and thin distributions compared to light mesons. Mesons with heavy quark and anti-quark masses show distributions spread in higher \mathbf{k}_\perp values along with narrower distributions in x . From Fig. 3, it is observed that η_b has higher distribution in \mathbf{k}_\perp than η_c due to the presence of heavy b quark

in it. However both D^+ and D_s mesons shows almost similar distributions. In case of B mesons, B_c meson shows quite different distribution than that of B^+ and B_c mesons. However both B^+ and B_c mesons show maximum distributions compared to other models. It is observed that dynamic chiral symmetry is less important for heavy mesons. For antiquark TMDs, distributions of these mesons can be obtained using the following relations [71]

$$f_M^q(x, \mathbf{k}_\perp) = f_M^{\bar{q}}(1-x, -\mathbf{k}_\perp). \quad (20)$$

The above relations obey the conservation of momentum i.e, the total longitudinal momentum fraction and transverse momenta of carried by the constituent of a mesons are unity and zero respectively.

We have also calculated the average momenta $\langle \mathbf{k}_\perp \rangle$ and $\langle \mathbf{k}_\perp^2 \rangle$ carried by the quark inside a mesons using the following expression

$$\langle \mathbf{k}_\perp^n \rangle = \frac{\int dx d^2 \mathbf{k}_\perp |\mathbf{k}_\perp^n| f_M^q(x, \mathbf{k}_\perp^2)}{\int dx d^2 \mathbf{k}_\perp f_M^q(x, \mathbf{k}_\perp^2)}, \quad (21)$$

where $n = 1$ and 2 . The calculated average $\langle \mathbf{k}_\perp \rangle$ and $\langle \mathbf{k}_\perp^2 \rangle$ values have been presented in Table II. It is observed that the mean transverse momenta $\langle \mathbf{k}_\perp \rangle$ of quark is minimum for the light mesons and it gradually increase with heavy quarks. It can be seen that η_B valence quark carries the highest $\langle \mathbf{k}_\perp \rangle$ due to the presence of b quark and anti-quark in it. The $\langle \mathbf{k}_\perp^2 \rangle$ value is smaller than $\langle \mathbf{k}_\perp \rangle$ for the mesons except η_b and B_c , clearly indicating a rare phenomena for heavy mesons. Similar kind of results have also been observed in the BSE model [70].

A. Parton Distribution Functions

The probability of finding the constituent quark of a meson as a function of longitudinal momentum fraction x is encoded in one-dimensional PDFs. In case of spin-0 pseudoscalar mesons, there is only $f^q(x)$ unpolarized PDF at the leading twist [33, 40]. The unpolarized $f^q(x)$ can be obtained by integrating the $f_M^q(x, \mathbf{k}_\perp^2)$ TMD over transverse momentum of quark as

$$f^q(x) = \int d^2 \mathbf{k}_\perp f_M^q(x, \mathbf{k}_\perp^2). \quad (22)$$

PDFs can be calculated from quark GPDs by limiting our GPDs to $\Delta_\perp = 0$, where Δ_\perp is difference between the transverse momentum of final and initial meson as

$$f^q(x) = H_{M_q}(x, 0, 0) \quad (23)$$

In our calculations, the unpolarized PDF obeys all the PDF sum rules [68, 72] which are given as follows

$$\int dx f^{q(\bar{q})}(x) = 1, \quad (24)$$

$$\sum_q \int dx (x f^q(x) + (1-x) f^{\bar{q}}(x)) = 1. \quad (25)$$

Here $f^{\bar{q}}$ is the anti-quark PDF. As in this work, we have not considered gluon contributions, therefore, the total momentum of a meson will be distributed between the quark and anti-quark. We have plotted the unpolarized $f^q(x)$ PDF for different mesons with respect to longitudinal momentum fraction x in Fig. 6. It is observed that the pion u -quark PDF distributes all over x and is symmetric about $x = 0.5$ along with η_c and η_b mesons. The quark PDFs of B mesons show maximum distribution in the range of $0 \leq x \leq 0.6$, whereas for the case of D -mesons the distributions lie in the range $0.4 \leq x \leq 1$. This clearly indicates that light quark of heavy mesons shows PDF distribution towards lower x and heavy quark of heavy mesons towards higher x . We have also evolved our pion and kaon constituent quark PDFs to $Q^2 = 16 \text{ GeV}^2$ using next to leading order (NLO) Dokshitzer-Gribov-Lipatov-Altarelli-Parisi a (DGLAP) equations using Brute-Force method [73–76]. The initial scale of our model is $Q_0^2 = 0.20 \text{ GeV}^2$. The evolved u -quark PDF has been presented Fig. 7 (a) with available modified FNAL-E615 experimental data [77]. Our predictions are found to be consistent with the experimental data. As there is no experimental data available for kaon PDF, we have compared our u - and s -quark PDFs of kaon with BLFQ predictions [43] and with Ref. [44] and presented the results of u - and s -quark PDFs of kaon in Figs. 7 (b) and (c) respectively. We observe that u -quark PDF of kaon vanishes after $x = 0.8$ unlike in the case of BLFQ. Similar kind of observations were obtained in Ref. [44]. The s -anti-quark PDF shows higher distributions as compared the u -quark, which has also been observed in Ref. [44, 78]. The kaon PDFs shows similar kind of distribution with other extractions [78] and model predictions [38, 79].

Further, we have calculated the average longitudinal momentum $\langle x \rangle$ carried by the quark from its parent mesons as $\langle x \rangle = \int dx x f^q(x)$. The calculated $\langle x \rangle$ values at the model scale have been presented in Table. II. We observe that the quark PDF of mesons with maximum difference of quark and anti-quark masses carry very less momentum compared to other mesons where the difference of the masses is small. This indicates that $\langle x \rangle$ of quark PDF is inversely proportional to

Mesons	LCQM (This work)				BSE model [70]
	$\langle \mathbf{k}_\perp \rangle$ (GeV)	$\langle \mathbf{k}_\perp^2 \rangle$ (GeV ²)	$\langle x \rangle$	$\langle x^{-1} \rangle$	$\langle \mathbf{k}_\perp \rangle$ (GeV)
$\pi^+(u\bar{d})$	0.328	0.1395	0.50	2.634	0.39
$K^+(u\bar{s})$	0.334	0.143	0.42	3.140	-
$\eta_c(c\bar{c})$	0.602	0.462	0.50	2.127	0.65
$\eta_B(b\bar{b})$	1.201	1.839	0.50	2.062	1
$D^+(c\bar{d})$	0.426	0.232	0.71	1.459	0.43
$D_s(c\bar{s})$	0.677	0.458	0.27	1.543	-
$B^+(u\bar{b})$	0.510	0.331	0.15	10.013	0.42
$B_s(s\bar{b})$	0.554	0.391	0.17	1.211	-
$B_c(c\bar{b})$	0.790	0.794	0.29	3.780	0.65

TABLE II: The average quark momenta $\langle \mathbf{k}_\perp \rangle$ and $\langle \mathbf{k}_\perp^2 \rangle$, average longitudinal quark momenta $\langle x \rangle$, inverse momenta $\langle x^{-1} \rangle$ for all the mesons. The BSE results [70] for $\langle \mathbf{k}_\perp \rangle$ have also been presented for comparison.

mass difference of quark and anti-quark. We have also calculated the inverse momenta as [68, 80]

$$\langle x^{-1} \rangle = \int dx x^{-1} f^q(x). \quad (26)$$

The inverse moment value of these mesons have also been presented in Table II. These inverse moments play an important role in describing the sum rules. It is observed that $\langle x^{-1} \rangle$ is maximum and minimum for B^+ and B_s respectively.

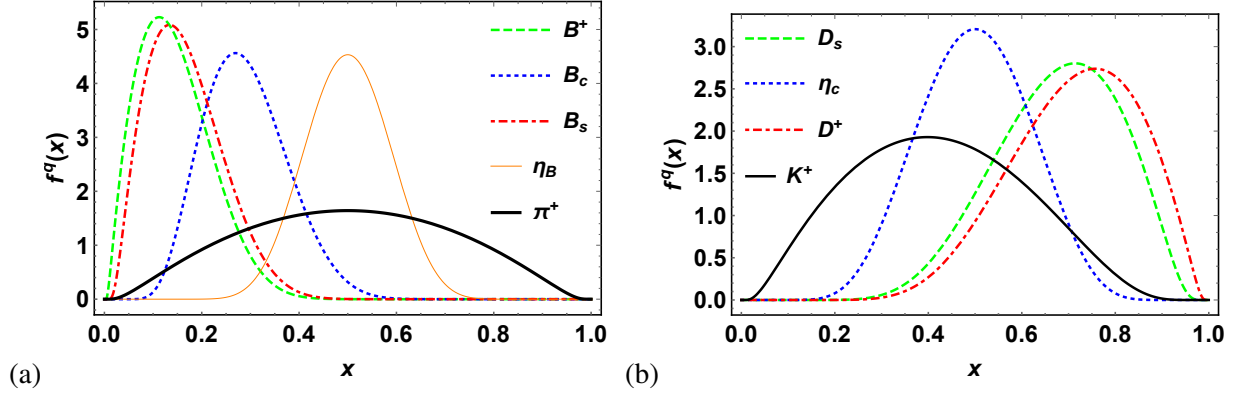


FIG. 6: (Color online) Unpolarized quark PDFs as a function of longitudinal momentum fraction x for different mesons.

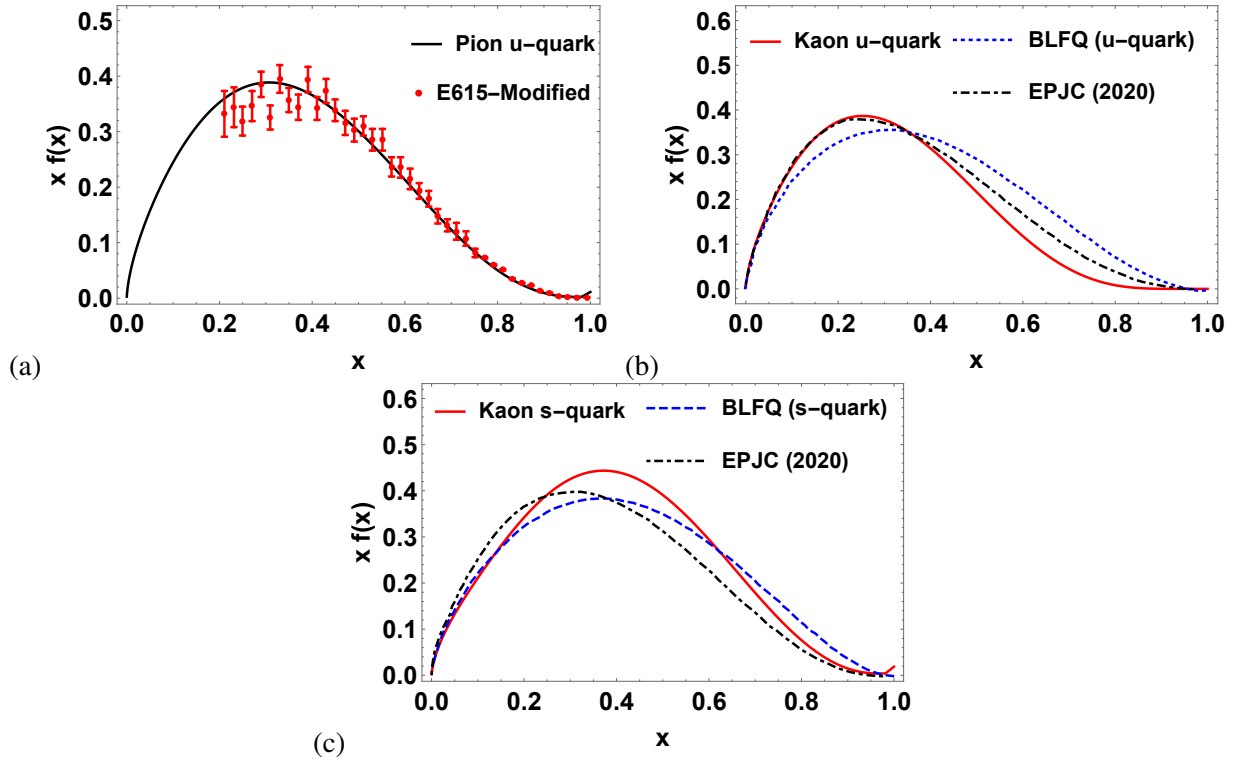


FIG. 7: (Color online) (a) pion u -quark PDF has been evolved to 16 GeV^2 from an initial scale of 0.20 GeV^2 and compared with modified FNAL-E615 data [77]. In (b) and (c), we have plotted the kaon u -quark and s -quark PDFs at 16 GeV^2 along with the BLFQ prediction data [43] and data in Ref. [44].

IV. GENERALIZED PARTON DISTRIBUTION FUNCTIONS

The matrix elements of quark operators at a light-like separation are defined as GPDs [12]. For spin-0 particles, we have only one chiral-even unpolarized GPD which can be defined in terms of the bilocal current as

$$H_M(x, \zeta, -t) = \frac{1}{2} \int \frac{dz^-}{2\pi} e^{ix\bar{P}^+z^-} \left\langle M(P', \lambda') \left| \bar{\Theta}\left(-\frac{z}{2}\right) \gamma^+ \Theta\left(\frac{z}{2}\right) \right| M(P, \lambda) \right\rangle. \quad (27)$$

Other kinematic variables which include the four-momentum transfer and skewness parameter are respectively expressed as $\Delta^\mu = P'^\mu - P^\mu$ with $t - \Delta^2 = -\Delta_\perp^2$ and $\zeta = -\Delta^+/2P^+$. We have chosen light-front gauge as $A^+ = 0$ which in turn makes gauge link, appearing between the quark field operators, unity. The overlap form of GPD $H_{M_q}(x, 0, -t)$ with zero skewness can be expressed as

$$\begin{aligned} H_M(x, 0, -t) = & \int \frac{d^2\mathbf{k}_\perp}{16\pi^3} [\Psi_{S_z=0}^*(x'', \mathbf{k}'_\perp, \uparrow, \uparrow) \Psi_{S_z=0}(x', \mathbf{k}'_\perp, \uparrow, \uparrow) \\ & + \Psi_{S_z=0}^*(x'', \mathbf{k}'_\perp, \uparrow, \downarrow) \Psi_{S_z=0}(x', \mathbf{k}'_\perp, \uparrow, \downarrow) + \Psi_{S_z=0}^*(x'', \mathbf{k}'_\perp, \downarrow, \uparrow) \Psi_{S_z=0}(x', \mathbf{k}'_\perp, \downarrow, \uparrow) \\ & + \Psi_{S_z=0}^*(x'', \mathbf{k}'_\perp, \downarrow, \downarrow) \Psi_{S_z=0}(x', \mathbf{k}'_\perp, \downarrow, \downarrow)], \end{aligned} \quad (28)$$

where \mathbf{k}'_\perp and \mathbf{k}'_\perp correspond to the final and initial state quark momentum respectively. In symmetric frame, they can be expressed as

$$\begin{aligned} \mathbf{k}'_\perp &= \mathbf{k}_\perp - (1 - x'') \frac{\Delta_\perp}{2}, \\ \mathbf{k}'_\perp &= \mathbf{k}_\perp + (1 - x') \frac{\Delta_\perp}{2}. \end{aligned} \quad (29)$$

Since we are dealing with zero skewness GPDs, the initial and final state longitudinal momentum fraction carried by an active quark of a meson remain the same. Hence, we can express initial and final state longitudinal momentum fraction by x only.

Fig. 8 presents the unpolarized GPDs for an active u -quark of π^+ and K^+ with respect to longitudinal momentum fraction x and invariant momentum transfer $-t$. It is observed that the distributions for both the mesons are intense at $-t = 0$ and fall off smoothly with an increase in the value of $-t$. However, the difference in these mesons lies in the peak values of x . The peak of the distribution for the case of K^+ is found to be shifted towards smaller values of x with tapering down of its x -dependence as compared to that for the π^+ distribution. This difference is a consequence of their respective antiquark masses. The massive \bar{s} antiquark of K^+ carries comparatively more longitudinal momentum fraction as compared to the \bar{d} antiquark of π^+ .

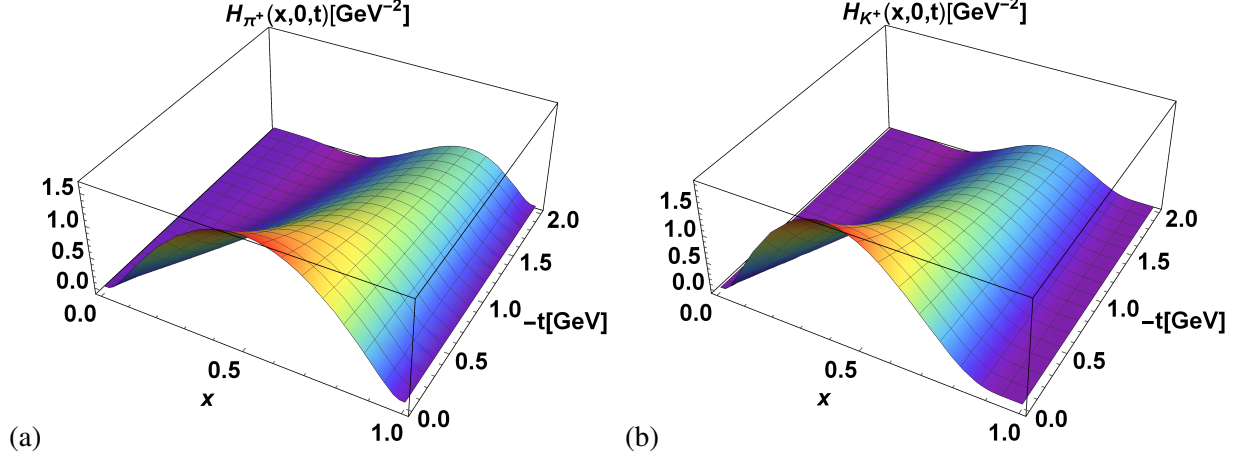


FIG. 8: (Color online) Unpolarized generalized parton distributions as a function of longitudinal momentum fraction x and invariant momentum transfer $-t$ for an active u -quark of (a) π^+ and (b) K^+ .

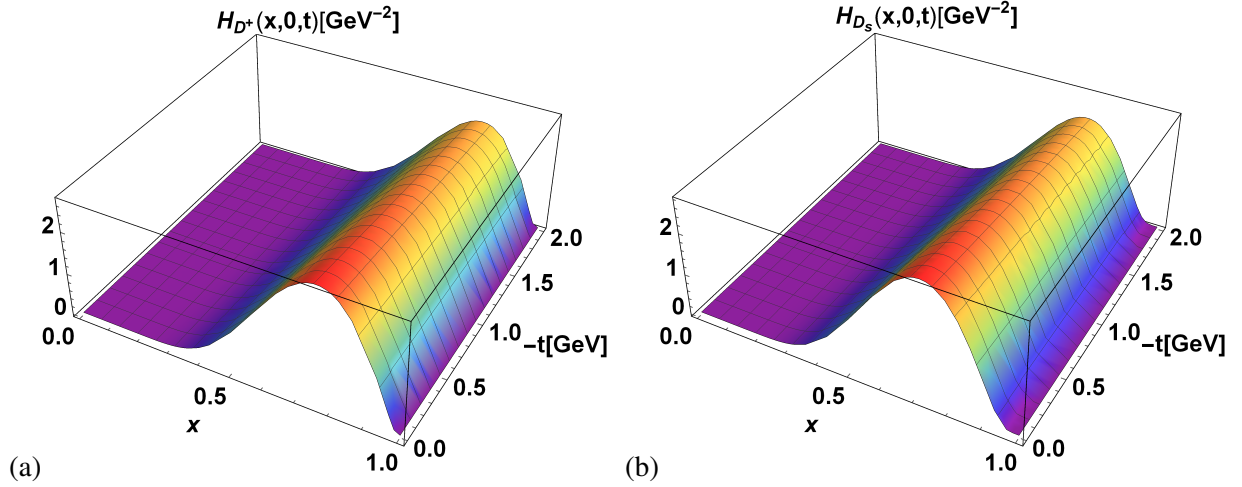


FIG. 9: (Color online) Unpolarized generalized parton distributions as a function of longitudinal momentum fraction x and invariant momentum transfer $-t$ for an active c -quark of (a) D^+ and (b) D_s mesons.

The unpolarized GPDs for an active c -quark of D mesons (D^+ and D_s) with respect to longitudinal momentum fraction x and invariant momentum transfer $-t$ are presented in Fig. 9. As in the case of light mesons, the distributions are intense at $-t = 0$. However, the distributions get tapered over a smaller region of x with no significant fall off with respect to $-t$ for both the D mesons. The

presence of peak value in the higher region of x as well as insignificant difference of peak values of x , for both D^+ and D_s mesons, can be attributed to the heavy mass of an active c -quark. In the same context, the distributions of unpolarized GPDs for active quarks of B mesons with respect to x and $-t$ are demonstrated in Fig. 10. Moving from a lighter B^+ meson to a comparatively heavier B_s meson and the heaviest B_c meson, the \bar{b} antiquark remains the same. However, the quark content changes from u to s and then c , respectively. With the increase in the mass of an active quark, the distributions are shifted to a comparatively larger values of x for zero momentum transfer with attenuation of fall off with respect to $-t$. Hence, the family of B mesons also approves the dependency of these distributions on quark masses. Among η_{c1} and η_b mesons, the unpolarized GPDs for their active quarks are also investigated to analyze the impact of mass on the ability to carry longitudinal momentum fraction x with and without momentum transfer $-t$. Their distributions show symmetric distribution around $x = 0.5$ as both quark-antiquark flavors are identical, hence having an equal probability of carrying longitudinal momentum fraction. However, the tapering down of distribution over a smaller region of x with almost negligible dependency on $-t$ for heavier b -quark flavor is also observed in Fig. 11. In short, the tapered x -dependence of distributions for heavy mesons implies less significance for dynamical chiral symmetry breaking for them. Distributions corresponding to unpolarized antiquark of a particular meson can be analyzed by replacing x by $(1 - x)$ in Eq. (28).

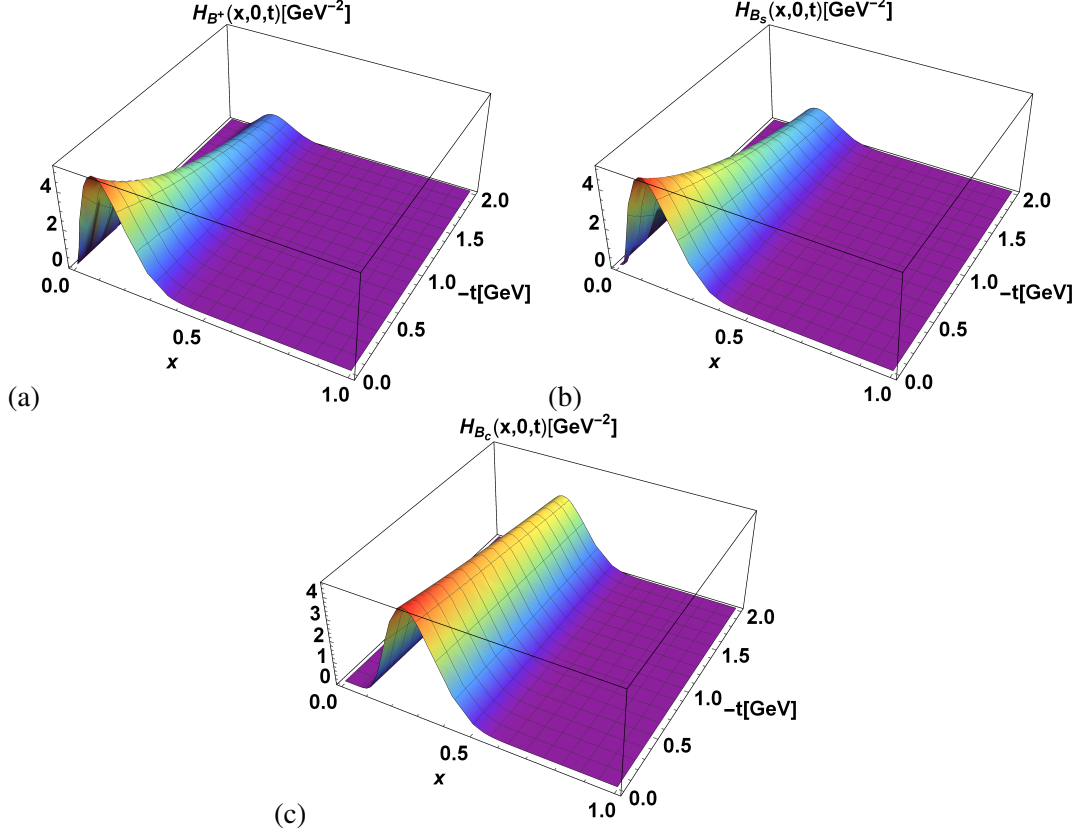


FIG. 10: (Color online) Unpolarized generalized parton distributions as a function of longitudinal momentum fraction x and invariant momentum transfer $-t$ for (a) an active u -quark of B^+ meson, (b) an active s -quark of B_s meson and (c) an active c -quark of B_c meson.

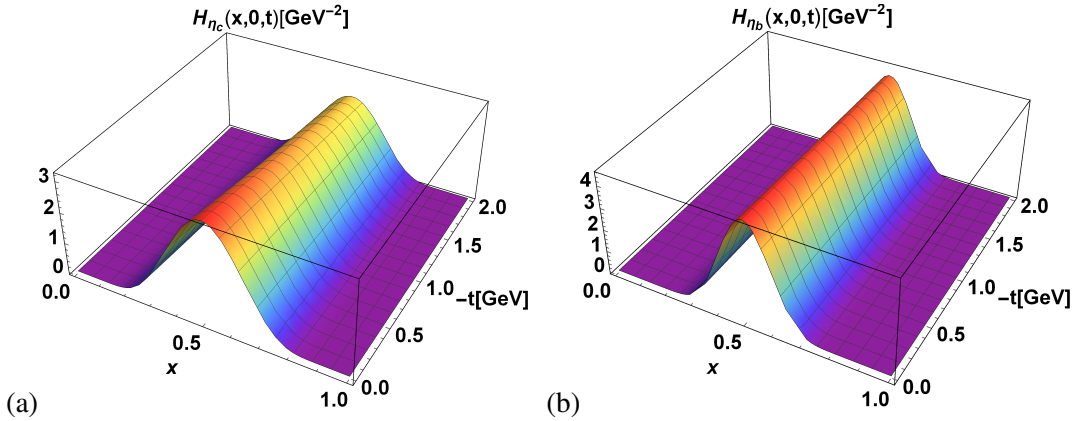


FIG. 11: (Color online) Unpolarized generalized parton distributions as a function of longitudinal momentum fraction x and invariant momentum transfer $-t$ for an active c -quark of (a) η_c and active b -quark of (b) η_b mesons.

V. FORM FACTORS

The zeroth moment of the unpolarized GPD $H_M(x, 0, -t)$ provides an insight to the contribution of q -quark flavor to the total elastic EMFF of meson and can be described as

$$F_{M_q}(-t) = \int dx H_M(x, 0, -t), \quad (30)$$

where $Q^2 = -t$. An analogous expression can be written for the meson antiquark, whereas complete EMFF of a meson can be obtained by summing up the charge multiplied form factors of constituent quark and antiquark of a meson as

$$F_M(-t) = e_q F_{M_q}(-t) + e_{\bar{q}} F_{M_{\bar{q}}}(-t). \quad (31)$$

EMFFs for quark-antiquark pairs carrying the same or comparatively lighter quarks than their antiquark partners are presented in Fig. 12 (a). A fast declination is found for EMFFs with an increase of Q^2 and a saturation near zero value of $|F_M(-t)|$. On the other hand, EMFFs for quark-antiquark pairs carrying the same or comparatively heavier quarks than their antiquark partners are presented in Fig. 12 (b), representing a smooth fall off of EMFFs with Q^2 . Between η_c and η_b , the fall of EMFF for η_c comes out to be steeper than η_b , which is a result of the mass difference between them. Heavier the quark, more gradually it will fall. Among D^+ , D_s and B_c mesons, $D^+ = c\bar{d}$ and $D_s = c\bar{s}$ show a similar behavior whereas the fall in $B_c = c\bar{b}$ is steeper. This is a consequence of the mass difference between the quark-antiquark pair and the EMFFs fall off more smoothly with Q^2 when the mass difference of its quark-antiquark pair is smaller.

A comparison of EMFFs for π^+ and K^+ with available data is presented in Fig. 13. Our model result for the case of pion overlaps with the available experimental data of JLab [81] for $1.5 < Q^2 < 2.5$ region very well. In addition, our results are also found to be within the error bars of other available data points of lattice and experimental data [82–86]. For K^+ meson, data is available only for smaller region of Q^2 are our results are in good agreement with the available data [87, 88]. The ratio between the kaon and pion form factor has been portrayed in Fig. 14, which shows compatible results to the experimental data [88]. However, in Ref. [89], the ratio between the kaon and pion form factor has a positive slope, which is in contradiction with our result with a negative slope of this ratio. For few heavier mesons, lattice data [90–92] is available for invariant momentum transfer $Q^2 < 2$ and the compatible comparison of our results with them are presented with them in Fig. 15 and 16 for D and η_c mesons.

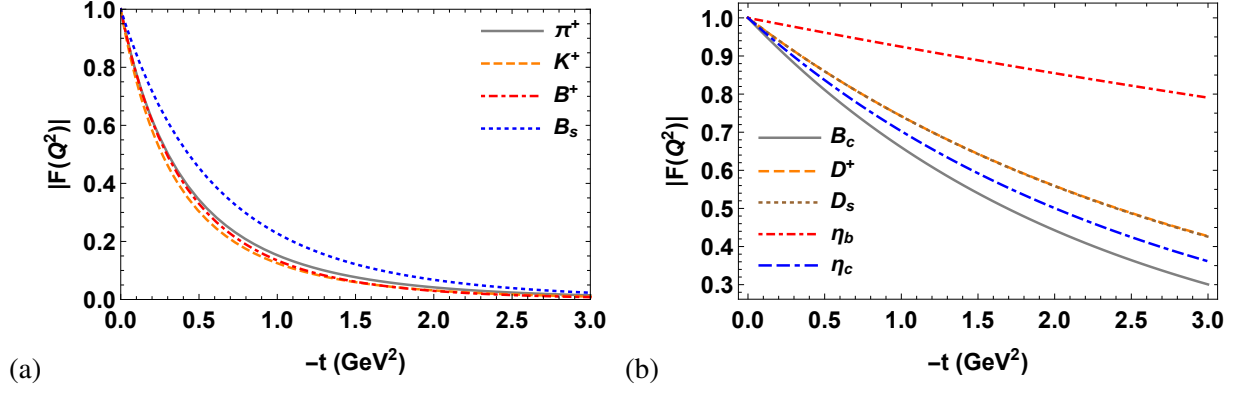


FIG. 12: (Color online) Electromagnetic form factors as a function of $-t$ for quarks of (a) light-light and light-heavy pair of mesons and (b) heavy-light and heavy-heavy pair of mesons.

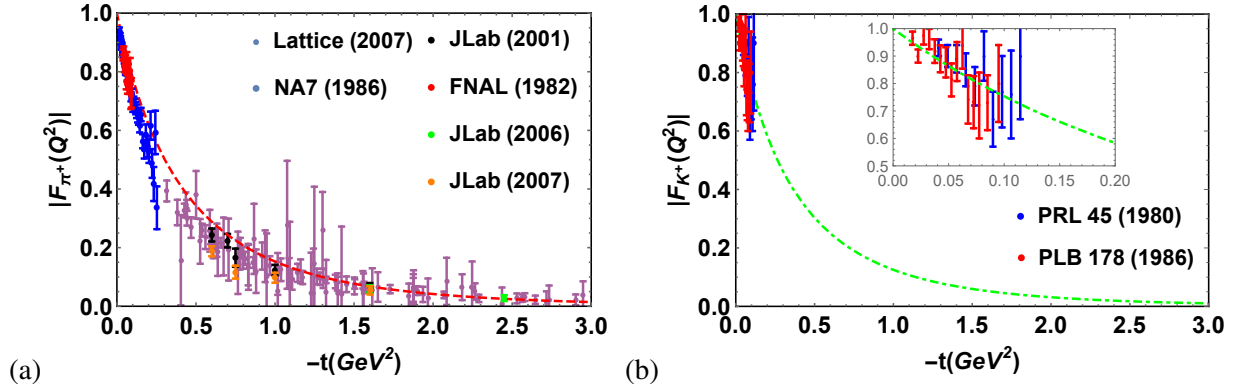


FIG. 13: (Color online) Electromagnetic form factors of (a) pion compared with NA7 [82], FNAL [83], lattice simulation [84], JLab (2001) [85], JLab (2006) [81], JLab (2007) [86] and (b) kaon compared with the available experimental data [87, 88].

The first moment of the unpolarized GPD $H_M(x, 0, -t)$ provides an insight to the contribution of the q -quark flavor to the total GFF of meson and can be described as

$$A_{2(M_q)}(-t) = \int dx x H_M(x, 0, -t). \quad (32)$$

Analogous to the EMFF of mesons, one can also obtain the GFF of mesons as expressed in Eq. (31). Both EMFFs and GFF obey the FF sum rules

$$F_M(Q^2 = 0) = 1, \quad (33)$$

$$A_{2(M_q)}(Q^2 = 0) + A_{2(M_{\bar{q}})}(Q^2 = 0) = 1. \quad (34)$$

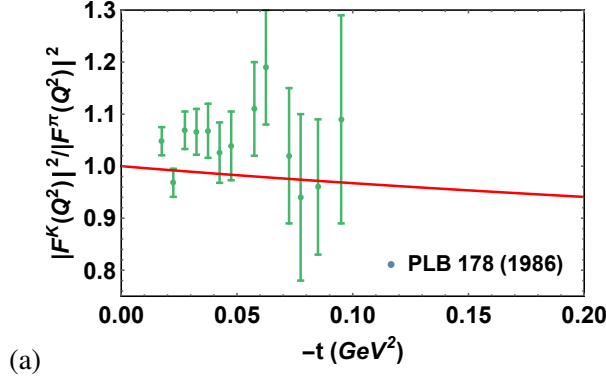


FIG. 14: (Color online) Electromagnetic form factors ratio of kaon to pion compared with the available experimental data [88].

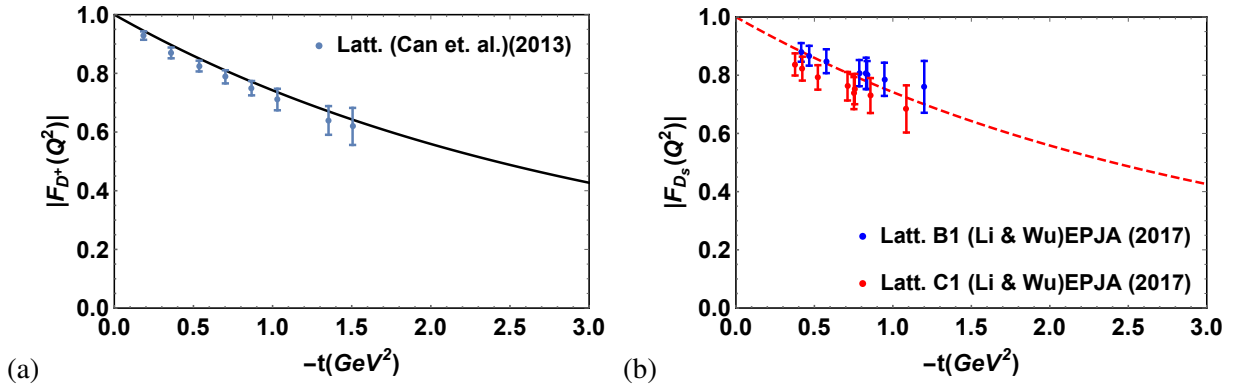


FIG. 15: (Color online) Electromagnetic form factors for an active u -quark of (a) D^+ compared with lattice simulation [90] and (b) D_s compared with available lattice data [91].

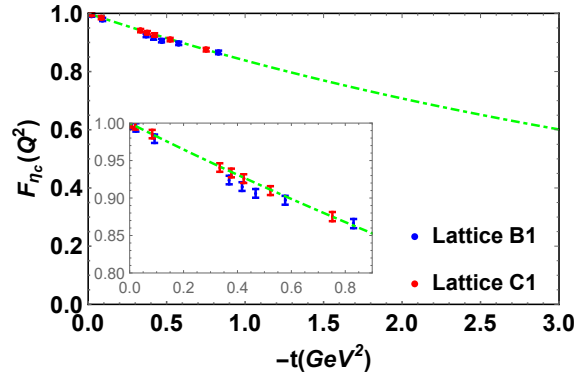


FIG. 16: (Color online) Electromagnetic form factors for an active c -quark of η_c compared with available data [92].

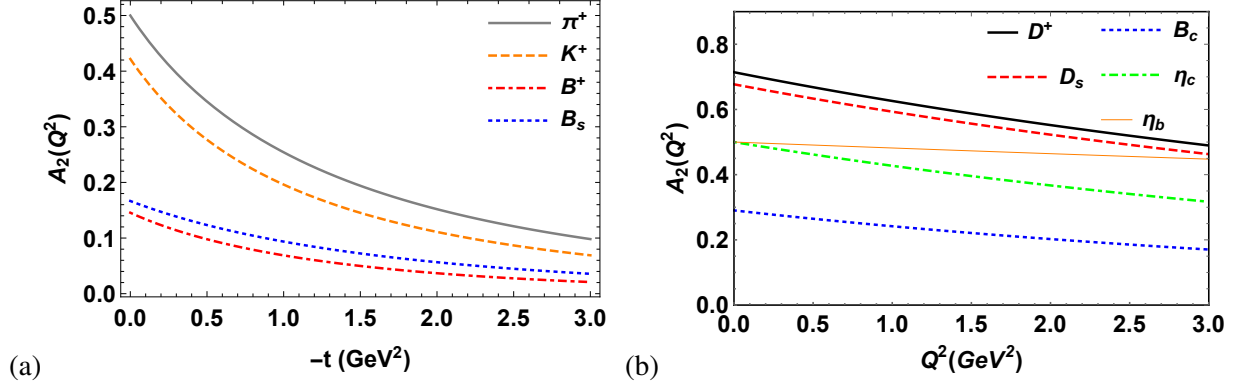


FIG. 17: (Color online) Gravitational form factors as a function of $-t$ for quarks of (a) light-light and light-heavy pair of mesons and (b) heavy-light and heavy-heavy pair of mesons.

GFFs of light-light and light-heavy pairs of mesons have been presented in Fig. 17 (a). They reflect that both light-light pseudoscalars follow same pattern of fall off with different amplitudes. This is a consequence of massive mass of \bar{s} in K^+ . Hence, more massive the quark, more is its contribution towards meson's total EMFF. Similar kind of trend is only seen between contribution of valence quarks of B^+ and B_s mesons. Fig. 17 (b) represents the GFFs of heavy-light and heavy-heavy pairs of mesons. η_b and η_c mesons have same $A_Q(0)$ values but η_c shows a significant fall off with $-t$ as compared to that in than η_b . D^+ and D_s represent a steeper trend with $-t$ when compared to η_c mesons but with higher amplitudes. As we move from D^+ to D_s meson, the mass difference between the quark-antiquark of a meson decreases, thus the amplitude of $A_c(-t)$. Further, B_c meson has the least amplitude of $A_c(-t)$ as it contains smallest mass difference between the quark-antiquark pair than D^+ and D_s . In short, the amplitude of the GFFs of mesons decreases as the mass of the quark of a meson carrying same quark-antiquark flavor decreases or the mass difference between quark-antiquark pairs decreases.

VI. SUMMARY

We have considered the light-cone quark model to study the transverse and spatial structure of spin-0 light as well as heavy pseudoscalar mesons. Quark quark correlator has been solved in the light-cone framework to study the transverse momentum dependent distributions (TMDs) and generalized parton distributions (GPDs). Three-dimensional valence quark distributions of unpolarized TMD $f_1(x, \mathbf{k}_\perp)$ as a function of longitudinal momentum fraction x and transverse

momentum \mathbf{k}_\perp implies a dependence of light pseudoscalar mesons on entire region of x with abrupt fall off with increase in \mathbf{k}_\perp . However, heavy pseudoscalar mesons are found to show x dependence on comparatively smaller region with a very smooth fall off with \mathbf{k}_\perp . From unpolarized TMD, an average momenta $\langle \mathbf{k}_\perp \rangle$ and $\langle \mathbf{k}_\perp^2 \rangle$ carried by the active quark inside mesons are also computed. These values are found to increase gradually as mesons becomes heavy. Except η_b and B_c mesons, the value of $\langle \mathbf{k}_\perp^2 \rangle$ for all other considered light and heavy mesons comes out to be less than $\langle \mathbf{k}_\perp \rangle$. Parton distribution functions are also evaluated from their unpolarized TMDs for all the pseudoscalar mesons. These distributions reveal that as the quark becomes heavy, the probability of finding the constituent quark with comparatively higher x is more. Evolved distributions are found to be compatible with available experimental data for pion and BLFQ predictions for kaon valence partons. Average longitudinal momentum $\langle x \rangle$ carried by the active quark from its parent meson is inversely proportional to the mass difference of quark-antiquark pair.

Three-dimensional valence quark distributions of chiral-even unpolarized generalized parton distribution as a function of longitudinal momentum fraction x and invariant momentum transfer $-t$ are also studied. The general trend of intense distributions at zero transverse momentum transfer is same for all the light as well as heavy pseudoscalar mesons. However, the peak value of distributions for heavy mesons is shifted to comparatively larger values of x with tapering down of distributions over x -dependence. An attenuated fall off for the distributions with $-t$ is also observed. Narrowed distributions over x reflect minimal impact of dynamical chiral symmetry breaking in heavy mesons. Furthermore, electromagnetic form factors (EMFFs) and gravitational form factors (GFFs) are also investigated. For pions, sufficient experimental and lattice simulated data is available and our results come out to be compatible with them. Kaon and ratio of kaon to pion EMFFs are also compared with the available data for small values of $-t$ which are also in good agreement. For the case of D^+ , D_s and η_c mesons, only lattice simulated data is available and we found compatible results of EMFFs for them. Comparison of EMFFs among all light and heavy pseudoscalar follows: lighter the active quark, more steeper is the EMFF distribution for it. Similar behavior is also followed by GFFs of active quarks of mesons. However, amplitude of GFFs depends merely on the mass of the constituent quark of a meson.

VII. ACKNOWLEDGEMENT

H.D. would like to thank the Science and Engineering Research Board, Anusandhan-National Research Foundation, Government of India under the scheme SERB-POWER Fellowship (Ref No. SPF/2023/000116) for financial support.

VIII. REFERENCE

- [1] S. J. Brodsky, H.-C. Pauli, and S. S. Pinsky, Quantum chromodynamics and other field theories on the light cone, *Phys. Rept.* **301**, 299 (1998), arXiv:hep-ph/9705477.
- [2] W.-M. Zhang, A Weak coupling treatment of nonperturbative QCD dynamics to heavy hadrons, *Phys. Rev. D* **56**, 1528 (1997), arXiv:hep-ph/9705226.
- [3] J. C. Collins and D. E. Soper, Parton Distribution and Decay Functions, *Nucl. Phys. B* **194**, 445 (1982).
- [4] A. D. Martin, R. G. Roberts, W. J. Stirling, and R. S. Thorne, Parton distributions: A New global analysis, *Eur. Phys. J. C* **4**, 463 (1998), arXiv:hep-ph/9803445.
- [5] M. Gluck, E. Reya, and A. Vogt, Dynamical parton distributions of the proton and small x physics, *Z. Phys. C* **67**, 433 (1995).
- [6] S. Alekhin, Parton distributions from deep inelastic scattering data, *Phys. Rev. D* **68**, 014002 (2003), arXiv:hep-ph/0211096.
- [7] J. Polchinski and M. J. Strassler, Deep inelastic scattering and gauge / string duality, *JHEP* **05**, 012, arXiv:hep-th/0209211.
- [8] M. Diehl, Introduction to GPDs and TMDs, *Eur. Phys. J. A* **52**, 149 (2016), arXiv:1512.01328 [hep-ph].
- [9] R. Angeles-Martinez *et al.*, Transverse Momentum Dependent (TMD) parton distribution functions: status and prospects, *Acta Phys. Polon. B* **46**, 2501 (2015), arXiv:1507.05267 [hep-ph].
- [10] B. Pasquini, S. Cazzaniga, and S. Boffi, Transverse momentum dependent parton distributions in a light-cone quark model, *Phys. Rev. D* **78**, 034025 (2008), arXiv:0806.2298 [hep-ph].
- [11] N. Kaur, S. Puhan, R. Pandey, A. Kumar, S. Dutt, and H. Dahiya, Does nuclear medium affect the transverse momentum-dependent parton distributions of valence quark of pions?, (2024),

- arXiv:2409.05394 [hep-ph].
- [12] M. Diehl, Generalized parton distributions, *Phys. Rept.* **388**, 41 (2003), arXiv:hep-ph/0307382.
- [13] J. M. M. Chavez, V. Bertone, F. De Soto Borrero, M. Defurne, C. Mezrag, H. Moutarde, J. Rodríguez-Quintero, and J. Segovia, Pion generalized parton distributions: A path toward phenomenology, *Phys. Rev. D* **105**, 094012 (2022), arXiv:2110.06052 [hep-ph].
- [14] J.-L. Zhang and J.-L. Ping, Kaon generalized parton distributions and light-front wave functions in the Nambu–Jona-Lasinio model, *Eur. Phys. J. C* **81**, 814 (2021).
- [15] W. Broniowski, V. Shastry, and E. Ruiz Arriola, Off-shell generalized parton distributions and form factors of the pion, *Phys. Lett. B* **840**, 137872 (2023), arXiv:2211.11067 [hep-ph].
- [16] N. Kaur and H. Dahiya, Generalized parton distributions for the lowest-lying octet baryons, *Eur. Phys. J. A* **60**, 42 (2024), arXiv:2310.03462 [hep-ph].
- [17] M. Guidal, M. V. Polyakov, A. V. Radyushkin, and M. Vanderhaeghen, Nucleon form-factors from generalized parton distributions, *Phys. Rev. D* **72**, 054013 (2005), arXiv:hep-ph/0410251.
- [18] M. G. Echevarria, P. A. Gutierrez Garcia, and I. Scimemi, GTMDs and the factorization of exclusive double Drell-Yan, *Phys. Lett. B* **840**, 137881 (2023), arXiv:2208.00021 [hep-ph].
- [19] S. Meissner, A. Metz, and M. Schlegel, Generalized parton correlation functions for a spin-1/2 hadron, *JHEP* **08**, 056, arXiv:0906.5323 [hep-ph].
- [20] K. Goeke, A. Metz, and M. Schlegel, Parameterization of the quark-quark correlator of a spin-1/2 hadron, *Phys. Lett. B* **618**, 90 (2005), arXiv:hep-ph/0504130.
- [21] A. Bacchetta, F. Delcarro, C. Pisano, M. Radici, and A. Signori, Extraction of partonic transverse momentum distributions from semi-inclusive deep-inelastic scattering, Drell-Yan and Z-boson production, *JHEP* **06**, 081, [Erratum: *JHEP* 06, 051 (2019)], arXiv:1703.10157 [hep-ph].
- [22] Y. Makris, F. Ringer, and W. J. Waalewijn, Joint thrust and TMD resummation in electron-positron and electron-proton collisions, *JHEP* **02**, 070, arXiv:2009.11871 [hep-ph].
- [23] D. Boer, R. Jakob, and P. J. Mulders, Asymmetries in polarized hadron production in $e^+ e^-$ annihilation up to order $1/Q$, *Nucl. Phys. B* **504**, 345 (1997), arXiv:hep-ph/9702281.
- [24] S. Catani, D. de Florian, G. Ferrera, and M. Grazzini, Vector boson production at hadron colliders: transverse-momentum resummation and leptonic decay, *JHEP* **12**, 047, arXiv:1507.06937 [hep-ph].
- [25] N. Kaur and H. Dahiya, Transverse distortion and single-spin asymmetries for low-lying octet baryons, *Int. J. Mod. Phys. A* **39**, 2450076 (2024), arXiv:2405.00445 [hep-ph].

- [26] A. Freese and I. C. Cloët, Quark spin and orbital angular momentum from proton generalized parton distributions, *Phys. Rev. C* **103**, 045204 (2021), arXiv:2005.10286 [nucl-th].
- [27] X. Luan and Z. Lu, Generalized parton distributions of sea quark at zero skewness in the light-cone model, *Eur. Phys. J. C* **83**, 504 (2023), arXiv:2302.11278 [hep-ph].
- [28] X.-D. Ji, Deeply virtual Compton scattering, *Phys. Rev. D* **55**, 7114 (1997), arXiv:hep-ph/9609381.
- [29] G. Xie, W. Kou, Q. Fu, Z. Ye, and X. Chen, Deeply virtual compton scattering at future electron-ion colliders, *Eur. Phys. J. C* **83**, 900 (2023), arXiv:2306.02357 [hep-ph].
- [30] L. Favart, M. Guidal, T. Horn, and P. Kroll, Deeply Virtual Meson Production on the nucleon, *Eur. Phys. J. A* **52**, 158 (2016), arXiv:1511.04535 [hep-ph].
- [31] W. Brooks, I. Schmidt, and M. Siddikov, Deeply virtual meson production on neutrons, *Phys. Rev. D* **98**, 116006 (2018), arXiv:1810.08077 [hep-ph].
- [32] S. Meissner, A. Metz, M. Schlegel, and K. Goeke, Generalized parton correlation functions for a spin-0 hadron, *JHEP* **08**, 038, arXiv:0805.3165 [hep-ph].
- [33] N. Kaur and H. Dahiya, Transverse momentum dependent parton distributions of pion in the light-front holographic model, *Int. J. Mod. Phys. A* **36**, 2150052 (2021), arXiv:1908.08657 [hep-ph].
- [34] M. Cerutti, L. Rossi, S. Venturini, A. Bacchetta, V. Bertone, C. Bissolotti, and M. Radici (MAP (Multi-dimensional Analyses of Partonic distributions)), Extraction of pion transverse momentum distributions from Drell-Yan data, *Phys. Rev. D* **107**, 014014 (2023), arXiv:2210.01733 [hep-ph].
- [35] M.-H. Chu *et al.* (Lattice Parton), Transverse-momentum-dependent wave functions of the pion from lattice QCD, *Phys. Rev. D* **109**, L091503 (2024), arXiv:2302.09961 [hep-lat].
- [36] M. Engelhardt, P. Hägler, B. Musch, J. Negele, and A. Schäfer, Lattice QCD study of the Boer-Mulders effect in a pion, *Phys. Rev. D* **93**, 054501 (2016), arXiv:1506.07826 [hep-lat].
- [37] B. Pasquini and P. Schweitzer, Pion transverse momentum dependent parton distributions in a light-front constituent approach, and the Boer-Mulders effect in the pion-induced Drell-Yan process, *Phys. Rev. D* **90**, 014050 (2014), arXiv:1406.2056 [hep-ph].
- [38] C. Han, G. Xie, R. Wang, and X. Chen, An Analysis of Parton Distribution Functions of the Pion and the Kaon with the Maximum Entropy Input, *Eur. Phys. J. C* **81**, 302 (2021), arXiv:2010.14284 [hep-ph].
- [39] W. Kou, C. Shi, X. Chen, and W. Jia, Transverse momentum dependent parton distributions of pion at leading twist, *Phys. Rev. D* **108**, 036021 (2023), arXiv:2304.09814 [hep-ph].

- [40] S. Puhan, S. Sharma, N. Kaur, N. Kumar, and H. Dahiya, T-even TMDs for the spin-0 pseudo-scalar mesons upto twist-4 using light-front formalism, *JHEP* **02**, 075, arXiv:2310.03464 [hep-ph].
- [41] S. Puhan and H. Dahiya, Leading twist T-even TMDs for the spin-1 heavy vector mesons, *Phys. Rev. D* **109**, 034005 (2024), arXiv:2310.03465 [hep-ph].
- [42] J.-H. Zhang, J.-W. Chen, L. Jin, H.-W. Lin, A. Schäfer, and Y. Zhao, First direct lattice-QCD calculation of the x -dependence of the pion parton distribution function, *Phys. Rev. D* **100**, 034505 (2019), arXiv:1804.01483 [hep-lat].
- [43] J. Lan, C. Mondal, S. Jia, X. Zhao, and J. P. Vary, Pion and kaon parton distribution functions from basis light front quantization and QCD evolution, *Phys. Rev. D* **101**, 034024 (2020), arXiv:1907.01509 [nucl-th].
- [44] Z.-F. Cui, M. Ding, F. Gao, K. Raya, D. Binosi, L. Chang, C. D. Roberts, J. Rodríguez-Quintero, and S. M. Schmidt, Kaon and pion parton distributions, *Eur. Phys. J. C* **80**, 1064 (2020).
- [45] F. E. Serna, B. El-Bennich, and G. a. Krein, Parton distribution functions and transverse momentum dependence of heavy mesons, (2024), arXiv:2409.01441 [hep-ph].
- [46] B. Almeida-Zamora, J. J. Cobos-Martínez, A. Bashir, K. Raya, J. Rodríguez-Quintero, and J. Segovia, Algebraic model to study the internal structure of pseudoscalar mesons with heavy-light quark content, *Phys. Rev. D* **109**, 014016 (2024), arXiv:2309.17282 [hep-ph].
- [47] S. Puhan and H. Dahiya, Spatial and Transverse structure of Heavy B- and D-mesons, *PoS HQL2023*, 089 (2024), arXiv:2408.07717 [hep-ph].
- [48] R. Acharyya, S. Puhan, N. Kumar, and H. Dahiya, Spectroscopy of excited quarkonium states in the light-front quark model, (2024), arXiv:2408.07715 [hep-ph].
- [49] J.-W. Chen, H.-W. Lin, and J.-H. Zhang, Pion generalized parton distribution from lattice QCD, *Nucl. Phys. B* **952**, 114940 (2020), arXiv:1904.12376 [hep-lat].
- [50] S. Kaur, N. Kumar, J. Lan, C. Mondal, and H. Dahiya, Tomography of light mesons in the light-cone quark model, *Phys. Rev. D* **102**, 014021 (2020), arXiv:2002.01199 [hep-ph].
- [51] N. Kaur, N. Kumar, C. Mondal, and H. Dahiya, Generalized Parton Distributions of Pion for Non-Zero Skewness in AdS/QCD, *Nucl. Phys. B* **934**, 80 (2018), arXiv:1807.01076 [hep-ph].
- [52] R. Abdul Khalek *et al.*, Science Requirements and Detector Concepts for the Electron-Ion Collider: EIC Yellow Report, *Nucl. Phys. A* **1026**, 122447 (2022), arXiv:2103.05419 [physics.ins-det].
- [53] B. Adams *et al.*, Letter of Intent: A New QCD facility at the M2 beam line of the CERN SPS (COMPASS++/AMBER), (2018), arXiv:1808.00848 [hep-ex].

- [54] A. J. Arifi, L. Happ, S. Ohno, and M. Oka, Structure of heavy mesons in the light-front quark model, *Phys. Rev. D* **110**, 014020 (2024), arXiv:2401.07933 [hep-ph].
- [55] H. J. Weber, Light cone quark model with spin force for the nucleon and Delta (1232), *Phys. Lett. B* **287**, 14 (1992).
- [56] B.-W. Xiao, X. Qian, and B.-Q. Ma, The Kaon form-factor in the light cone quark model, *Eur. Phys. J. A* **15**, 523 (2002), arXiv:hep-ph/0209138.
- [57] R. Acharyya, S. Puhan, and H. Dahiya, Quark spin-orbit correlations in spin-0 and spin-1 mesons using the light-front quark model, *Phys. Rev. D* **110**, 034020 (2024), arXiv:2405.00446 [hep-ph].
- [58] B.-W. Xiao and B.-Q. Ma, Pion photon and photon pion transition form-factors in the light cone formalism, *Phys. Rev. D* **68**, 034020 (2003), arXiv:hep-ph/0312162.
- [59] S. Puhan and H. Dahiya, Spatial and transverse structure of heavy b- and d-mesons, in *Proceedings of 16th International Conference on Heavy Quarks and Leptons — PoS(HQL2023)*, HQL2023 (Sissa Medialab, 2024) p. 089.
- [60] C. Shi, J. Li, M. Li, X. Chen, and W. Jia, Transverse momentum distributions of valence quarks in light and heavy vector mesons, *Phys. Rev. D* **106**, 014026 (2022), arXiv:2205.02757 [hep-ph].
- [61] G. P. Lepage and S. J. Brodsky, Exclusive Processes in Perturbative Quantum Chromodynamics, *Phys. Rev. D* **22**, 2157 (1980).
- [62] B. Pasquini, S. Rodini, and S. Venturini (MAP (Multi-dimensional Analyses of Partonic distributions)), Valence quark, sea, and gluon content of the pion from the parton distribution functions and the electromagnetic form factor, *Phys. Rev. D* **107**, 114023 (2023), arXiv:2303.01789 [hep-ph].
- [63] W. Qian and B.-Q. Ma, Vector meson omega-phi mixing and their form factors in light-cone quark model, *Phys. Rev. D* **78**, 074002 (2008), arXiv:0809.4411 [hep-ph].
- [64] S. J. Brodsky, M. Diehl, and D. S. Hwang, Light cone wave function representation of deeply virtual Compton scattering, *Nucl. Phys. B* **596**, 99 (2001), arXiv:hep-ph/0009254.
- [65] H. M. Choi and C.-R. Ji, Light cone quark model predictions for radiative meson decays, *Nucl. Phys. A* **618**, 291 (1997).
- [66] A. J. Arifi, H.-M. Choi, C.-R. Ji, and Y. Oh, Mixing effects on 1S and 2S state heavy mesons in the light-front quark model, *Phys. Rev. D* **106**, 014009 (2022), arXiv:2205.04075 [hep-ph].
- [67] A. Bacchetta, F. G. Celiberto, M. Radici, and P. Tael, Transverse-momentum-dependent gluon distribution functions in a spectator model, *Eur. Phys. J. C* **80**, 733 (2020), arXiv:2005.02288 [hep-ph].

- [68] C. Lorcé, B. Pasquini, and P. Schweitzer, Transverse pion structure beyond leading twist in constituent models, *Eur. Phys. J. C* **76**, 415 (2016), arXiv:1605.00815 [hep-ph].
- [69] C. Lorcé, B. Pasquini, and P. Schweitzer, Unpolarized transverse momentum dependent parton distribution functions beyond leading twist in quark models, *JHEP* **01**, 103, arXiv:1411.2550 [hep-ph].
- [70] C. Shi, P. Liu, Y.-L. Du, and W. Jia, Heavy flavor-asymmetric pseudoscalar mesons on the light front, (2024), arXiv:2409.05098 [hep-ph].
- [71] L. Albino, I. M. Higuera-Angulo, K. Raya, and A. Bashir, Pseudoscalar mesons: Light front wave functions, GPDs, and PDFs, *Phys. Rev. D* **106**, 034003 (2022), arXiv:2207.06550 [hep-ph].
- [72] Z. Zhu, Z. Hu, J. Lan, C. Mondal, X. Zhao, and J. P. Vary (BLFQ), Transverse structure of the pion beyond leading twist with basis light-front quantization, *Phys. Lett. B* **839**, 137808 (2023), arXiv:2301.12994 [hep-ph].
- [73] M. Miyama and S. Kumano, Numerical solution of Q^{*2} evolution equations in a brute force method, *Comput. Phys. Commun.* **94**, 185 (1996), arXiv:hep-ph/9508246.
- [74] M. Hirai, S. Kumano, and M. Miyama, Numerical solution of Q^{*2} evolution equations for polarized structure functions, *Comput. Phys. Commun.* **108**, 38 (1998), arXiv:hep-ph/9707220.
- [75] M. Hirai, S. Kumano, and M. Miyama, Numerical solution of Q^{*2} evolution equation for the transversity distribution $\Delta(T)q$, *Comput. Phys. Commun.* **111**, 150 (1998), arXiv:hep-ph/9712410.
- [76] M. Hirai and S. Kumano, Numerical solution of Q^2 evolution equations for fragmentation functions, *Comput. Phys. Commun.* **183**, 1002 (2012), arXiv:1106.1553 [hep-ph].
- [77] M. Aicher, A. Schafer, and W. Vogelsang, Soft-gluon resummation and the valence parton distribution function of the pion, *Phys. Rev. Lett.* **105**, 252003 (2010), arXiv:1009.2481 [hep-ph].
- [78] C. Bourrely, F. Buccella, W.-C. Chang, and J.-C. Peng, Extraction of kaon partonic distribution functions from Drell-Yan and J/ψ production data, *Phys. Lett. B* **848**, 138395 (2024), arXiv:2305.18117 [hep-ph].
- [79] K. D. Bednar, I. C. Cloët, and P. C. Tandy, Distinguishing Quarks and Gluons in Pion and Kaon Parton Distribution Functions, *Phys. Rev. Lett.* **124**, 042002 (2020), arXiv:1811.12310 [nucl-th].
- [80] S. J. Brodsky, F. J. Llanes-Estrada, and A. P. Szczepaniak, Illuminating the $1/x$ moment of parton distribution functions, *eConf* **C070910**, 149 (2007), arXiv:0710.0981 [nucl-th].
- [81] T. Horn *et al.* (Jefferson Lab F(pi)-2), Determination of the Charged Pion Form Factor at $Q^{*2} = 1.60$ and $2.45-(\text{GeV}/c)^{*2}$, *Phys. Rev. Lett.* **97**, 192001 (2006), arXiv:nucl-ex/0607005.

- [82] S. R. Amendolia *et al.* (NA7), A Measurement of the Space - Like Pion Electromagnetic Form-Factor, Nucl. Phys. B **277**, 168 (1986).
- [83] E. B. Dally *et al.*, Elastic Scattering Measurement of the Negative Pion Radius, Phys. Rev. Lett. **48**, 375 (1982).
- [84] D. Brömmel *et al.* (QCDSF/UKQCD), The Pion form-factor from lattice QCD with two dynamical flavours, Eur. Phys. J. C **51**, 335 (2007), arXiv:hep-lat/0608021.
- [85] J. Volmer *et al.* (Jefferson Lab F(pi)), Measurement of the Charged Pion Electromagnetic Form-Factor, Phys. Rev. Lett. **86**, 1713 (2001), arXiv:nucl-ex/0010009.
- [86] V. Tadevosyan *et al.* (Jefferson Lab F(pi)), Determination of the pion charge form-factor for $Q^2 = 0.60\text{-GeV}^2 - 1.60\text{-GeV}^2$, Phys. Rev. C **75**, 055205 (2007), arXiv:nucl-ex/0607007.
- [87] E. B. Dally *et al.*, DIRECT MEASUREMENT OF THE NEGATIVE KAON FORM-FACTOR, Phys. Rev. Lett. **45**, 232 (1980).
- [88] S. R. Amendolia *et al.*, A Measurement of the Kaon Charge Radius, Phys. Lett. B **178**, 435 (1986).
- [89] O. A. T. Dias, V. S. Filho, and J. P. B. C. de Melo, Kaon and Pion Electromagnetic Form Factor Ratios in the Light-Front, Nucl. Phys. B Proc. Suppl. **199**, 281 (2010), arXiv:1001.4039 [hep-ph].
- [90] K. U. Can, G. Erkol, M. Oka, A. Ozpineci, and T. T. Takahashi, Vector and axial-vector couplings of D and D* mesons in 2+1 flavor Lattice QCD, Phys. Lett. B **719**, 103 (2013), arXiv:1210.0869 [hep-lat].
- [91] N. Li and Y.-J. Wu, Lattice study of D and D_s meson form factors with twisted boundary conditions, Eur. Phys. J. A **53**, 56 (2017).
- [92] N. Li, C.-C. Liu, and Y.-J. Wu, Lattice study of form factors for charmonium, Eur. Phys. J. A **56**, 242 (2020).